Innate Stat3-mediated induction of the antimicrobial protein Reg3γ is required for host defense against MRSA pneumonia

Sun-Mi Choi,[1,2] Jeremy P. McAleer,[2] Mingquan Zheng,[2] Derek A. Pociask,[2] Mark H. Kaplan,[3] Shulin Qin,[4] Todd A. Reinhart,[4] and Jay K. Kolls[1,2]

[1]Department of Genetics, Louisiana State University Health Sciences Center, New Orleans, LA 70112
[2]Richard King Mellon Foundation Institute for Pediatric Research, Children's Hospital of Pittsburgh, Pittsburgh, PA 15224
[3]Herman B. Wells Center for Pediatric Research, Department of Pediatrics, Indiana University, Indianapolis, IN 46202
[4]Graduate School of Public Health, University of Pittsburgh, Pittsburgh, PA 15261

Pulmonary *Staphylococcus aureus* (SA) infections are a public health concern and a major complication of hyper-IgE syndrome, caused by mutations in STAT3. In contrast to previous findings of skin infection, we observed that clearance of SA from the lung did not require T, B, or NK cells but did require Stat3 activation. Immunohistochemistry showed robust Stat3 phosphorylation in the lung epithelium. We identified that a critical Stat3 target gene in lung epithelium is *Reg3g* (*regenerating islet-derived 3 γ*), a gene which is highly expressed in gastrointestinal epithelium but whose role in pulmonary host defense is uncharacterized. Stat3 regulated *Reg3g* transcription through direct binding at the *Reg3g* promoter region. Recombinant Reg3γ bound to SA and had both bacteriostatic and bactericidal activity in a dose-dependent fashion. Stat3 inhibition in vivo reduced *Reg3g* transcripts in the lung, and more importantly, recombinant Reg3γ rescued mice from defective SA clearance. These findings reveal an antibacterial function for lung epithelium through Stat3-mediated induction of Reg3γ.

CORRESPONDENCE
Jay K. Kolls:
Jay.Kolls@chp.edu

Abbreviations used: BALF, bronchoalveolar lavage fluid; ChIP, chromatin immunoprecipitation; HIES, hyper-IgE syndrome; Lif, leukemia inhibitory factor; MRSA, methicillin-resistant SA; MSSA, methicillin-sensitive SA; OA, oropharyngeal aspiration; qPCR, quantitative PCR; SA, *Staphylococcus aureus*; TSB, tryptic soy broth.

Staphylococcus aureus (SA) causes more infections worldwide than any other bacterial pathogen (DeLeo et al., 2010). 20–50% of healthy adult populations around the world are colonized with SA, including >89 million Americans (30% of the population). Of these, 2.3 million people are colonized with methicillin-resistant strains (Kuehnert et al., 2006; Defres et al., 2009). This opportunistic gram-positive bacterium can colonize epithelia such as the mucocutaneous nasopharynx, but clinical infection can occur upon a break in epidermal or mucosal integrity and/or a decline in immune defenses (Graham et al., 2006). In an immunocompromised host, severe life-threatening infections such as meningitis, endocarditis, and pneumonia can occur, causing significant morbidity and mortality (Klevens et al., 2007). Methicillin-resistant SA (MRSA) is no longer limited to hospitals and is found in 1–3% of the general population (Klevens et al., 2007). Pneumonia is the second leading site of invasive MRSA infection after bacteremia and can occur in previously healthy individuals (Napolitano et al., 2009; David and Daum, 2010).

The lung epithelium provides the first line of immune defense against pulmonary pathogens because of its structural barrier and mucociliary clearance mechanisms. In addition, the lung epithelium secretes various chemokines, cytokines, and antimicrobial proteins in response to bacterial pathogens (Bals and Hiemstra, 2004). Although adaptive immunity is important to clear MRSA in the skin of mice (Cho et al., 2010), B, T, and NK cells do not seem to be important in the lung because the bacteria are largely cleared by 48 h after infection and *Rag2*$^{-/-}$*IL2rγ*$^{-/-}$ mice are able to clear infection efficiently (Small et al., 2008; von Köckritz-Blickwede et al., 2008). Nevertheless, patients with inherited (autosomal dominant) hyper-IgE syndrome (HIES) are susceptible to recurrent SA pulmonary infections of the skin and lung as the result of loss-of-function mutations in STAT3

© 2013 Choi et al. This article is distributed under the terms of an Attribution–Noncommercial–Share Alike–No Mirror Sites license for the first six months after the publication date (see http://www.rupress.org/terms). After six months it is available under a Creative Commons License (Attribution–Noncommercial–Share Alike 3.0 Unported license, as described at http://creativecommons.org/licenses/by-nc-sa/3.0/).

The Rockefeller University Press $30.00
J. Exp. Med. 2013 Vol. 210 No. 3 551-561
www.jem.org/cgi/doi/10.1084/jem.20120260

The Journal of Experimental Medicine

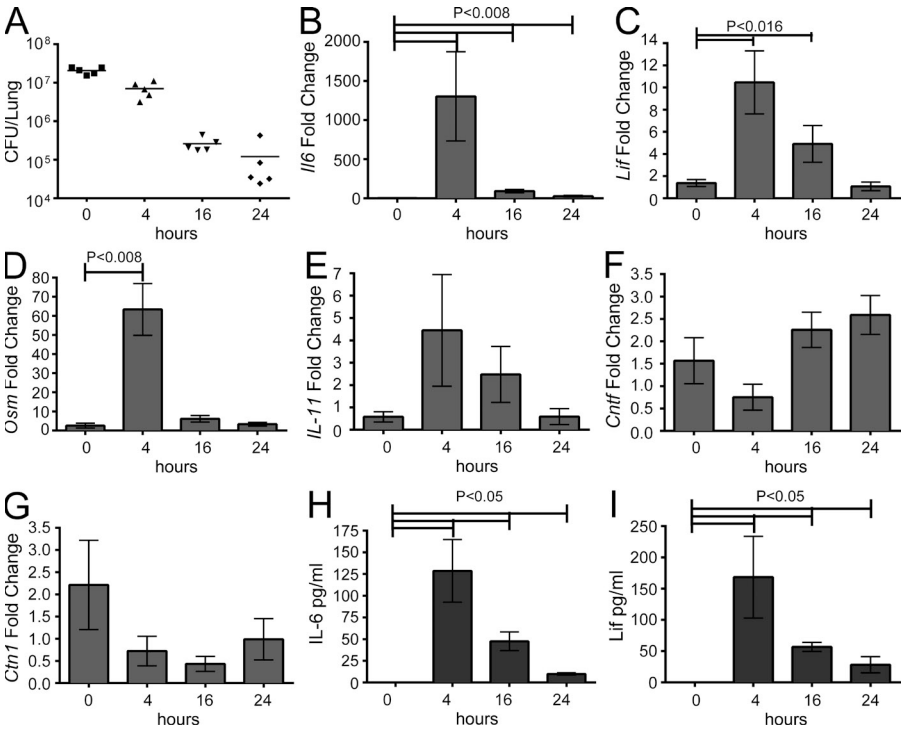

Figure 1. Gp130 ligands IL-6 and Lif are induced during MRSA pneumonia. (A–I) Quantification of MRSA lung burden (A), gene expression (B–G), and protein levels (H and I) 0, 4, 16, and 24 h after OA of USA300 (2×10^7 CFU). MRSA lung burden was determined by CFU assay, gene expression by qPCR of TaqMan probes, and protein levels by Luminex assay. Gene expression levels are normalized to *Hprt*. $n = 5$ in each group, independently performed three times. P-values by Mann-Whitney test are as indicated. Horizontal bars represent the mean of the data. Error bars represent the SE.

(Heimall et al., 2010). Phosphorylation of Stat3 can occur in response to the IL-6 family of cytokines through the IL-6 signal transducer (IL6ST) coreceptor, also known as Gp130. Phosphorylated Stat3 (P-Stat3) dimerizes, translocates to the nucleus, and transcriptionally modifies many genes. Stat3 is required for Th17 differentiation and T cell–dependent IgG responses; however, it is also involved in epithelial homeostasis, wound healing, and production of antimicrobial factors (i.e., β-defensins) in response to Staphylococcal and *Candida* infections (Quinton et al., 2008; Pickert et al., 2009). It has been shown that IL-17A and IL-22 within conditioned media from activated T cells induce keratinocytes to produce antimicrobial factors CXCL8 and β-defensin 2 and 3. Moreover, γδ T cell–derived IL-17 is important in controlling SA infection in the skin (Cho et al., 2010). In support of a role of IL-17 in cutaneous SA infection, supernatants from stimulated HIES T cells have lower amounts of IL-17 and IL-22 compared with non-HIES patients and fail to induce the antimicrobial factors CXCL8 and β-defensin 2 and 3 in keratinocytes, demonstrating that mutations in STAT3 lead to defects in antimicrobial production (Minegishi et al., 2009). Despite these data, the respective role of Stat3 signaling in hematopoietic versus nonhematopoietic cells in controlling the susceptibility to SA pulmonary infection remains unclear. Preliminary evidence for a role of nonmyeloid Stat3 in the increased susceptibility of pulmonary SA infection in HIES patients is supported by a case of an unsuccessful bone marrow transplant in an HIES patient that failed to control recurrent SA infections (Gennery et al., 2000). Based on these data, we hypothesized that nonhematopoietic cell Stat3 signaling is required for host defense against MRSA in the lung.

Similar to prior published findings (Small et al., 2008; von Köckritz-Blickwede et al., 2008), we found that clearance of MRSA (USA300) in a mouse model of SA pneumonia was independent of B, T, and NK cells. However, clearance was defective in mice in which Stat3 was inhibited or deleted in lung epithelial cells. These data demonstrate that nonhematopoietic Stat3 is critical for host defense in MRSA lung infection. We found that Stat3 regulated the expression of Reg3γ (regenerating islet-derived 3 γ), which is highly expressed in the lung epithelium during MRSA infection. Moreover, *Reg3g* induction was independent of B, T, and NK cells but dependent on Gp130-induced Stat3 signaling. We detected both full-length and cleaved forms of Reg3γ in the bronchoalveolar lavage fluid (BALF) after MRSA pneumonia, and recombinant full-length Reg3γ showed dose-dependent bacteriostatic activity against USA300, whereas the cleaved form showed bactericidal activity. Neutralization of Reg3γ in vivo perturbed clearance of MRSA in the lung. Furthermore, in vivo administration of recombinant Reg3γ restored mucosal immunity against MRSA. Collectively, we have shown that MRSA initiates induction of antimicrobial Reg3γ by pulmonary epithelial cells in a Stat3-dependent manner and epithelial Stat3 is critical for clearance of MRSA in the lung. Recombinant Reg3γ may be a novel way to augment mucosal immunity to this infection.

RESULTS

Gp130 ligands IL-6 and leukemia inhibitory factor (Lif) are induced in MRSA pneumonia

We developed a model of MRSA pneumonia and conducted time course experiments to assess bacterial clearance and potential

activators of the Stat3 signaling pathway. Oropharyngeal aspiration (OA) of C56BL/6 (WTB6) mice with 2×10^7 CFU of USA300 showed time-dependent clearance of the organism with clearance of 99% of the bacteria by 24 h after infection (Fig. 1 A). To determine the host immune defenses against MRSA, lung mRNA and protein were obtained and analyzed for levels of cytokines and chemokines. Transcripts for the Gp130 ligands *Il6*, *Lif*, and *Osm* were increased in the lung and were highest at 4 h after infection (Fig. 1, B–D). IL-6 and Lif protein levels were also increased in lung homogenates 4 h after infection (Fig. 1, H and I). This induction was not true for all Gp130 ligands, as transcripts for *Cntf* and *Ctn1* were not increased by MRSA pneumonia (Fig. 1, F and G).

T, B, and NK cells are dispensable for pulmonary MRSA clearance

To localize the cells of Stat3 activation and determine which cells are important for MRSA clearance, USA300 infection was performed in various immunological KO mice. In agreement with previous studies (Small et al., 2008; von Köckritz-Blickwede et al., 2008), pulmonary MRSA clearance was not dependent on T, B, and NK cells, as $Rag2^{-/-}/Il2r\gamma^{-/-}$ mice cleared USA300 similarly to WTB6 mice at 20 h after infection (Fig. 2 A). As expected, the induction of *Il17a* and *Il22* was absent in $Rag2^{-/-}/Il2r\gamma^{-/-}$ mice (not depicted); however, the induction of *Il6*, the primary Gp130 ligand, was unaffected in $Rag2^{-/-}/Il2r\gamma^{-/-}$ mice (Fig. 2 B). Moreover, clearance of USA300 was unaffected in $Il17ra^{-/-}$ and $Il22^{-/-}$ mice (Fig. 2 C). In support of a role of innate immunity in the pulmonary clearance of USA300, macrophages or neutrophils were depleted in WTB6 mice by clodronate or 1A8 antibody, respectively. OA administration of clodronate depleted >90% of $CD11c^+$ cells (not depicted) and resulted in a 2-log increase in lung CFU compared with mice receiving vehicle control (Fig. 2 D). Using FACS and intracellular staining for IL-6, the bulk of IL-6 at 4 h after USA300 infection was in $F480^+$ macrophages (Fig. 2 E). Consistent with this, the induction of IL-6 was dependent on macrophages as clodronate administration decreased the BALF levels of IL-6 at 4 h after infection (Fig. 2 F). Depletion of neutrophils also exacerbated MRSA clearance by one-half log but was not as significant as macrophage depletion (Fig. 2 D).

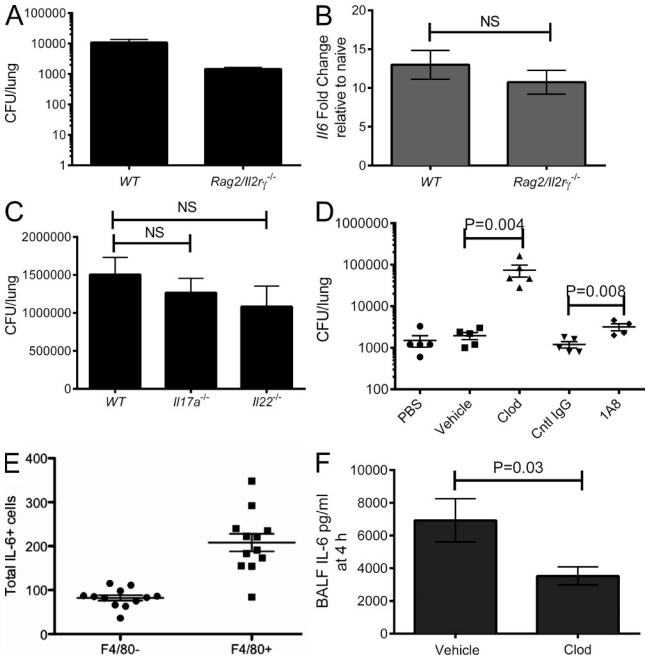

Figure 2. T, B, and NK cells are dispensable for IL-6 induction and MRSA pneumonia clearance. (A) WT C57BL/6 and $Rag2^{-/-}/Il2r\gamma^{-/-}$ mice were OA administered 3×10^7 CFU of USA300, and lung burden by CFU counts was determined at 24 h after infection. (B) *Il6* gene expression of the lung was quantified by qPCR, values are normalized to *Hprt*, and fold change is relative to naive $Rag2^{-/-}/Il2r\gamma^{-/-}$ mice. $n = 5$ in each group, independently performed twice. (C) WTB6, $IL\text{-}17ra^{-/-}$, and $IL\text{-}22^{-/-}$ mice were OA administered 2×10^7 CFU of USA300. Lung burden by CFU counts was determined at 16 h after infection. $n = 5$ in each group, independently performed twice. (D) WT mice were depleted of macrophages or neutrophils by OA clodronate administration 48 h before infection or i.p. 1A8 antibody administration 24 h before infection, respectively. (E) Lung burden by CFU counts was determined at 24 h after infection. IL-6 intracellular staining in $F480^-$ versus $F480^+$ cells in the lung 4 h after USA300 ($n = 12$). (F) BALF IL-6 was analyzed by ELISA (BD) at 4 h after infection in clodronate- and control vehicle liposome–administered mice. $n = 5$ in each group, independently performed once. P-values by Mann-Whitney test are as indicated. Error bars represent the SE.

MRSA clearance is dependent on Gp130 and Stat3 signaling

Autosomal-dominant HIES is caused by mutations in STAT3 that prevent the activation of STAT3-inducible genes, leading to recurrent staphylococcal skin and pulmonary infections. Inhibition of Gp130 or Stat3 activation during MRSA pneumonia increased bacterial burden (Fig. 3). Local administration of an anti–mouse Gp130 neutralizing antibody immediately before MRSA infection significantly increased CFU at 18 h after infection (Fig. 3 A). To confirm the importance of Stat3 signaling in this model, we administered specific Stat3 inhibitors, JSI-124 or S3I-201, 1 h before MRSA infection. Both inhibitors increased MRSA lung burden 16 h after infection (Fig. 3, C and D). Moreover, both systemic (i.p.) and local (OA) routes of administration of S3I-201 resulted in increased bacterial burden at 16 h and 24 h, respectively (Fig. 3, B and C). Finally, JSI-124 inhibition of Stat3 signaling in $Rag2/Il2r\gamma^{-/-}$ mice also increased pulmonary MRSA burden at 16 h after infection (Fig. 3 E), demonstrating the critical role of Stat3 in WT mice as well as in mice that lack T, B, and NK cells.

Stat3 activation in airway epithelium is necessary for MRSA clearance

We detected basal P-Stat3 in naive mouse whole lung; however, there was a significant increase with MRSA infection (Fig. 4 A). To examine where Stat3 is activated during MRSA infection, we performed immunohistochemistry for P-Stat3 and noted that the lung epithelium was a major site of Stat3 activation upon MRSA infection (Fig. 4 B). Moreover, OA administration of the Stat3 inhibitor S3I-201 significantly

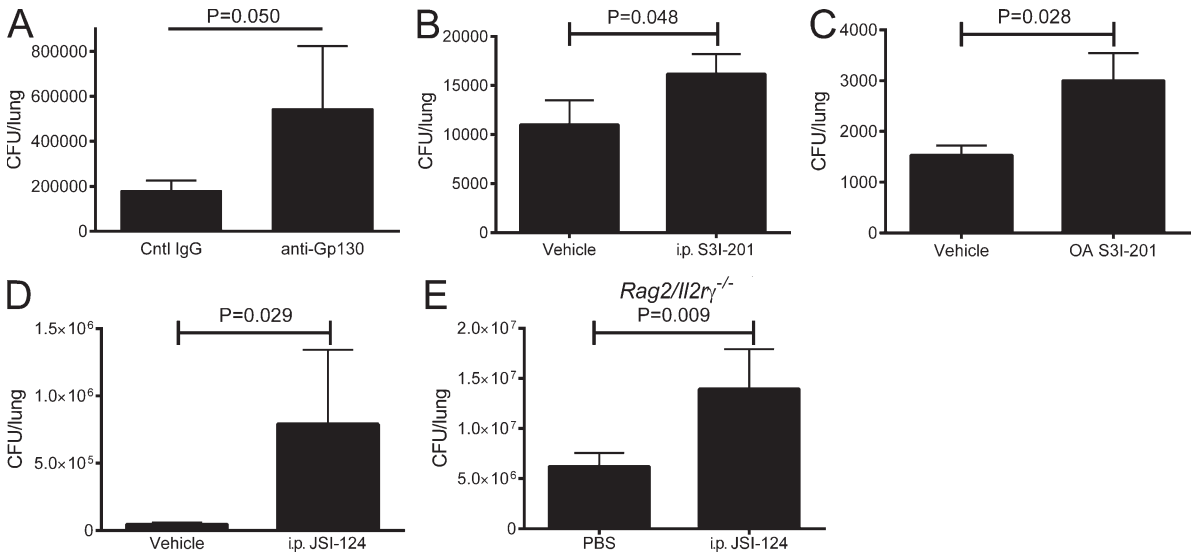

Figure 3. USA300 clearance is dependent on Gp130–induced Stat3 signaling. (A) Gp130 receptor was inhibited in WT mice by anti-Gp130 antibody given OA immediately before USA300 infection. n = 8–10 in each group. (B–D) Stat3 signaling was i.p. or OA inhibited by a small molecule inhibitor, S3I-201 (n = 5 in each group; B and C) or JSI-124 (n = 3 in each group; D), 1 h before OA USA300 infection. (A–E) Lung burden by CFU counts was determined 16 (A, B, D, and E) or 24 (C) h after infection. (E) Inhibition by i.p. JSI-124 of Stat3 signaling during MRSA pneumonia was also performed in *Rag2/Il2rγ*$^{-/-}$ mice. CFU bacterial lung burden was analyzed 16 h after infection. n = 9–11 in each group. All experiments were independently performed at least twice. P-values by Mann-Whitney test are as indicated. Error bars represent the SE.

reduced P-Stat3 staining with MRSA infection (Fig. 4, B and C). Because the lung epithelium was a major site of Stat3 activation, we next investigated whether epithelial Stat3 signaling was necessary for MRSA clearance. Adenoviral Cre (Ad-cre) or adenoviral luciferase (Ad-luc) was administered into the lung of *Stat3*$^{fl/fl}$ mice 6 d before MRSA challenge to deplete pulmonary epithelium of Stat3. Ad-cre targeting of lung epithelial cells significantly increased MRSA lung burden at 16 h after infection compared with control Ad-luc–treated control mice (Fig. 4 D). It is possible that epithelial Stat3 regulates antimicrobial factors in the lung that control clearance of USA300. To explore this possibility, we analyzed gene expression of known antimicrobial genes in a microarray dataset from Stat3$^{fl/fl}$ × SPC-cre mice (GEO accession no. GSE6846). Although calprotectin (S100A8/A9) is induced in the lung during MRSA infection (Fig. 5, A and B), analysis of microarray showed an increase of S100A8/A9 in Stat3-deficient mice, a phenotype which we also observed in USA300-infected mice administered a Stat3 inhibitor (Fig. 5, C and D). These data suggest that the increased expression of S100A8/A9 is not sufficient to compensate for Stat3 inhibition in clearance of USA300 in the lung. Moreover, USA300 failed to induce the expression of mouse β defensins 2 or 3 (not depicted), suggesting that these genes play a limited role in this model.

Reg3γ is induced in the lung during MRSA and limits MRSA growth in vitro

Xu et al. (2007) has reported that deletion of *Stat3* in pulmonary epithelial cells changes the expression of several growth factors and cytokines. Among these, *Reg3g* was highly repressed after *Stat3* deletion in surfactant protein C–positive cells (Matsuzaki et al., 2006; Xu et al., 2007). Consistent with Stat3 activation in the epithelium during pulmonary SA infection (Fig. 4), we found that *Reg3g* was expressed at a basal level followed by induction in whole lung tissue as early as 16 h after MRSA infection (Fig. 6 A). Reg3γ protein was induced in the lung as early as 4 h after USA300 infection (Fig. 6 B). Secreted Reg3γ was also detectable by Western blot on BALF taken at 20 h after infection (Fig. 6 C). In the BAL, we detected both full-length Reg3γ as well as cleaved Reg3γ as previously reported by Mukherjee et al. (2009; Fig. 6 C). Of note, protein levels of both IL-6 and Reg3γ were increased in naive *Rag2/IL2rg*$^{-/-}$ compared with WTB6 mice (Fig. 6, D and E), demonstrating that pulmonary Reg3γ expression is not dependent on cytokine products of T, B, or NK cells and may explain normal clearance of USA300 in this mouse strain. To determine whether Reg3γ has antibacterial activity against USA300, a recombinant fusion protein consisting of mouse Reg3γ and mouse IgG2a (Reg3γ-Fc; Zheng et al., 2008) was expressed in 293T cells and purified over protein G column. Reg3γ-Fc was capable of binding to live MRSA organisms (Fig. 6 F) and inhibited MRSA growth in nutrient-rich tryptic soy broth (TSB) media in a dose-dependent manner (Fig. 6 G). This protein had minimal binding to *Streptococcus pneumoniae* and minimal detectable binding to gram-negative bacteria including *Klebsiella pneumoniae*, *Haemophilus influenzae*, or *Moraxella catarrhalis* (Fig. 7 A). Reg3γ antibody neutralized the inhibition of MRSA growth by Reg3γ-Fc (Fig. 7 B). As we detected both full-length and cleaved forms of Reg3γ during MRSA infection and N-terminal cleaved Reg3γ has bactericidal activity against *Listeria monocytogenes* (Mukherjee et al., 2009),

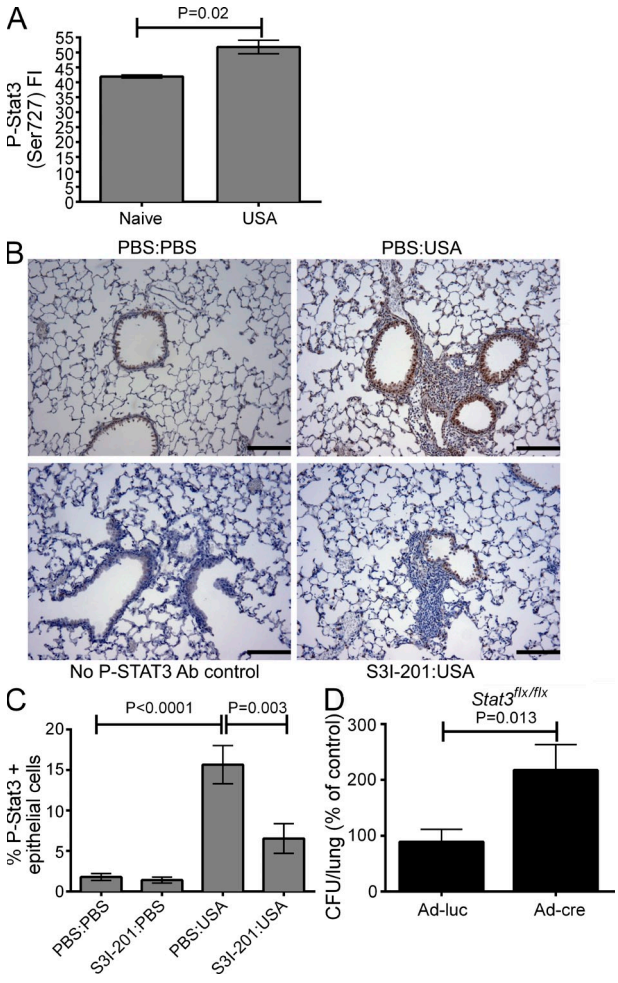

Figure 4. Stat3 activation in airway epithelium is necessary for MRSA clearance. (A) Phosphorylated Stat3 was detected in lung homogenates, naive and 20 h after USA300 infection by Luminex fluorescence intensity (FI). (B) P-Stat3 is localized to lung epithelium by immunohistochemistry. Bars, 200 µm. (C) The number of P-Stat3–positive cells from six random fields was counted in relation to the total number of epithelial cells in immunohistochemistry lung slides from naive, USA300-infected, and Stat3-inhibited-before-USA300-infection mice. $n = 5$ in each group. (D) Ad-cre was OA administered 6 d before USA300 challenge to deplete pulmonary epithelium of Stat3. CFU of USA300 lung burden was determined 16 h after infection. $n = 9$ in Ad-luc and $n = 11$ in Ad-cre groups, independently performed three times. P-values by Mann-Whitney test are as indicated. Error bars represent the SE.

we tested this protein against USA300. Similar to what has been reported for *L. monocytogenes* (Mukherjee et al., 2009), N terminal cleaved Reg3γ-C had bactericidal activity against USA300 (Fig. 7 C). Cleaved Reg3γ-C had no bactericidal activity against *K. pneumoniae*, *H. influenzae*, or *M. catarrhalis* (not depicted). Collectively, our data show that Reg3γ is induced in lung tissue after MRSA infection and that recombinant Reg3γ has potent growth-inhibitory activity against MRSA. These data are consistent with the earlier finding that Reg3γ has selective bactericidal activity against gram-positive organisms (Cash et al., 2006).

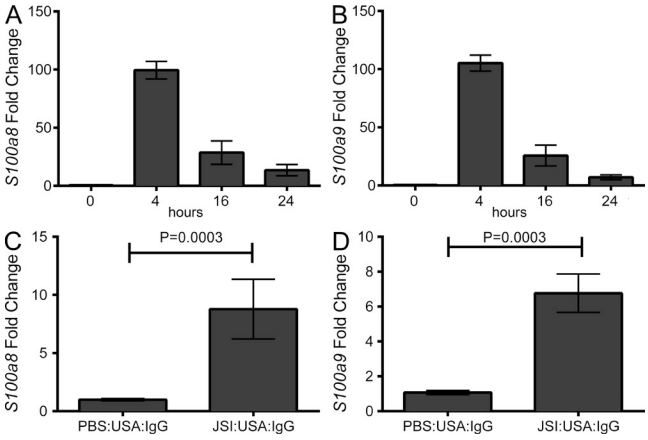

Figure 5. Expression of S100A8/A9. (A and B) Both *S100A8* (A) and *S100A9* (B) are induced in the lung during USA300 by real-time qPCR. (C and D) Consistent with genetic deletion of Stat3 in the epithelium, administration of JSI-124 increased expression of both *S100A8* (C) and *S100A9* (D) at 4 h after USA300 infection. $n = 5$ for each group. Error bars represent the SEM.

IL-6–stimulated P-Stat3 directly activates transcription of *Reg3g* in MLE12 cells

Because Gp130 signaling is required for MRSA clearance and the lung epithelium was a prominent site of Stat3 phosphorylation during USA300 infection, we analyzed IL-6 regulation of Reg3γ expression in lung epithelium using MLE12 cells. IL-6 stimulation of MLE12 cells increased P-Stat3 protein and induced functional Stat3-mediated transcription of a Stat3 luciferase reporter P-Stat3–luciferase MLE12 cell reporter line (Fig. 8, A and B). IL-6 also increased the level of *Reg3g* transcripts in these cells (Fig. 8 C). To determine whether P-Stat3 directly activates transcription of *Reg3g*, chromatin immunoprecipitation (ChIP) assays were performed on chromatin from IL-6–stimulated MLE12 cells using a P-Stat3 antibody. Stimulation with 50 ng/ml IL-22 was performed as a positive control as IL-22 stimulation of *Reg3g* is known to be Stat3 dependent (Zheng et al., 2008). Although there is a basal level of P-Stat3 binding to the *Reg3g* promoter, P-Stat3 binding was significantly enhanced by IL-6 and IL-22 stimulation (Fig. 8 D). Therefore, IL-6 production during MRSA pneumonia is capable of directly inducing Stat3 binding to the *Reg3g* locus in lung epithelial cells. We also observed induction of *Reg3g* in MLE12 cells by IFN-γ in vitro; however, USA300 was a weak inducer of IFN-γ protein in vivo compared with IL-6 (Fig. 8, E and F). Moreover, *Reg3g* was not induced by peptidoglycan, Pam3Cys, or LPS (not depicted).

Reg3g is induced in lung epithelium in response to MRSA USA300 in vivo, and recombinant Reg3γ rescues the defect in MRSA clearance with Stat3 inhibition

Consistent with these in vitro findings, *Reg3g* transcripts were localized to the lung epithelium during MRSA infection by in situ hybridization (Fig. 9 A). Moreover, *Reg3g* mRNA

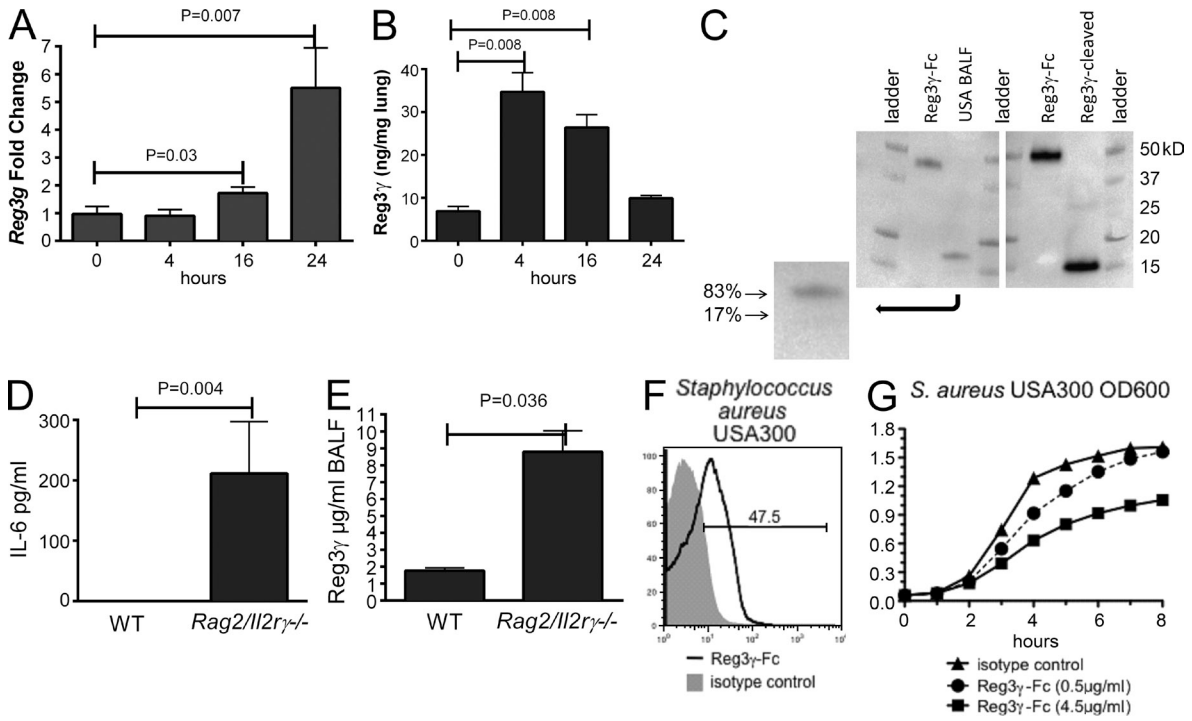

Figure 6. Reg3γ is induced in the lung during MRSA challenge and inhibits SA growth. (A) WTB6 mice were infected with USA300 and sacrificed at time 0, 4, 16, and 24 h. *Reg3g* expression was determined by real-time PCR and normalized to *Hprt*. $n = 5$ in each group, independently performed three times. (B) Reg3γ protein levels determined by ELISA on whole lung homogenates. (C) BALF was collected 20 h after USA300 infection, and Reg3γ was detected by Western blot (third lane), using recombinant Reg3γ-Fc (second and fifth lanes) and cleaved Reg3γ (sixth lane) proteins as controls. (D) Naive WTB6 and *Rag2/Il2rγ*$^{-/-}$ mice were euthanized, and 1 ml of BALF was obtained. IL-6 levels in lung homogenates were measured by Luminex. (E) BALF was analyzed for Reg3γ with a direct ELISA. $n = 5$ in each group. (F) USA300 was incubated with recombinant Reg3γ-mouse IgG2a-Fc fusion protein (Reg3γ-Fc) or isotype control, followed by incubation with a secondary anti-mouse IgG–Alexa Fluor 488 antibody. Shown is a representative histogram gated on live organisms. (G) USA300 was incubated with Reg3γ-Fc or isotype control, and OD600 readings were taken at hourly intervals. Assay was performed in triplicate, and results are representative of three independent experiments. P-values by Mann-Whitney test are as indicated. Error bars represent the SE.

expression during MRSA infection was attenuated by inhibition of Gp130/Stat3 signaling (Fig. 9, B–D). Because of the fact that *Reg3g*$^{-/-}$ mice have abnormal gut microflora (Vaishnava et al., 2011), which alters this strain's pulmonary immune response (unpublished observations), we chose to neutralize Reg3γ in vivo with intratracheal administration of anti-Reg3γ antibody. Anti-Reg3γ significantly increased lung CFUs of USA300 at 16 h after challenge (Fig. 9 E). This result was also confirmed by real-time quantitative PCR (qPCR) for SA normalized to GAPDH with a ΔCt of 1.24 ± 0.26 in the control antibody group versus a ΔCt of 14.12 ± 1.64 ($P < 0.005$ by Mann-Whitney test) in the anti-Reg3γ antibody group. Finally, local administration of recombinant Reg3γ-Fc 4 h after USA300 infection rescued the defect in MRSA clearance by Stat3 inhibition (Fig. 9 F), demonstrating a therapeutic role for Reg3γ. Collectively, Stat3 induces epithelial *Reg3g* in vivo, leading to the clearance of MRSA.

DISCUSSION

Although Reg3γ has been well described in the gastrointestinal system, to our knowledge this is the first study of functional Reg3γ protein in lung epithelium and its regulation in response to microbial challenge. Although multiple factors responsible for the induction of *Reg3g* transcription have been studied, this report of Gp130/Stat3 signaling in MLE12 cells as well as in the respiratory epithelium in mice suggests that *Reg3g* is a direct target of Stat3 in vitro and in vivo. The Reg3 family of lectins consists of Reg3α, Reg3β, and Reg3δ in addition to Reg3γ. Reg3β and Reg3γ are very similar in protein structure and are both induced during our model. However, in the in vitro OD600 growth curve experiment, recombinant Reg3β had no bacteriostatic activity against USA300 (unpublished data).

During SA skin infection, both IL-1r1 signaling and IL-17 production by T cells are necessary for host defense against SA (Miller et al., 2007; Cho et al., 2010). In this model, γδ T cells were an essential source of IL-17 and required for clearance of SA (Cho et al., 2010). In contrast, clearance of SA in the lung is fundamentally different, as *Rag2*$^{-/-}$*/Il2rγ*$^{-/-}$ mice clear SA similarly to WTB6 mice. Moreover, IL-17RA KO mice have similar SA lung burdens as WTB6 mice at 16 h after infection (Fig. 2 C). Therefore, different innate immune mechanisms are in play in lung and skin during SA infections.

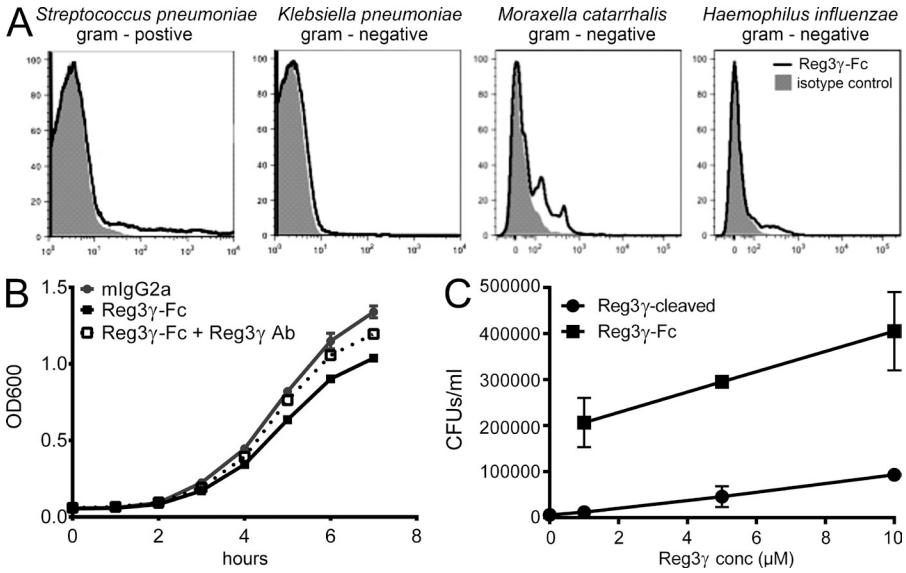

Figure 7. Reg3γ binding and bactericidal activity against USA300. (A) Reg3γ binding. Bacteria were incubated with recombinant Reg3γ-mouse IgG2a-Fc fusion protein (Reg3γ-Fc) or isotype control, followed by incubation with a secondary anti–mouse IgG–Alexa Fluor 488 antibody. (B and C) Anti-Reg3γ antibody neutralizes the bacteriostatic effect of Reg3γ-Fc, and cleaved Reg3γ is bactericidal against USA300. (B) USA300 was incubated with recombinant Reg3γ-mouse IgG2a-Fc fusion protein (Reg3γ-Fc), Reg3γ-Fc with Reg3γ antibody, or isotype control, and OD600 readings were taken at hourly intervals. (C) USA300 was incubated with varying concentrations of Reg3γ-Fc or cleaved Reg3γ for 2 h in 10 mM MES and 25 mM NaCl, pH 5.5, and plated for CFU analysis. Errors bars represent the SE.

Despite the lack of requirement for T, B, or NK cells, consistent with HIES patients, Stat3 was essential for optimal clearance of MRSA. Immunohistochemistry revealed that a major site of Stat3 phosphorylation is in the epithelium. Our present experiments do not exclude roles of Stat3 signaling in nonepithelial innate immune cells such as macrophages or neutrophils. Indeed, these cells are critical effector cells against SA. In fact, macrophages are a critical source of early IL-6 to activate Stat3 in this model. However, administration of Ad-cre to *Stat3*$^{fl/fl}$ mice, which deletes Stat3 in pulmonary epithelial cells, was sufficient to disrupt clearance of USA300. Although IL-22 is capable of mediating Stat3 in lung epithelium

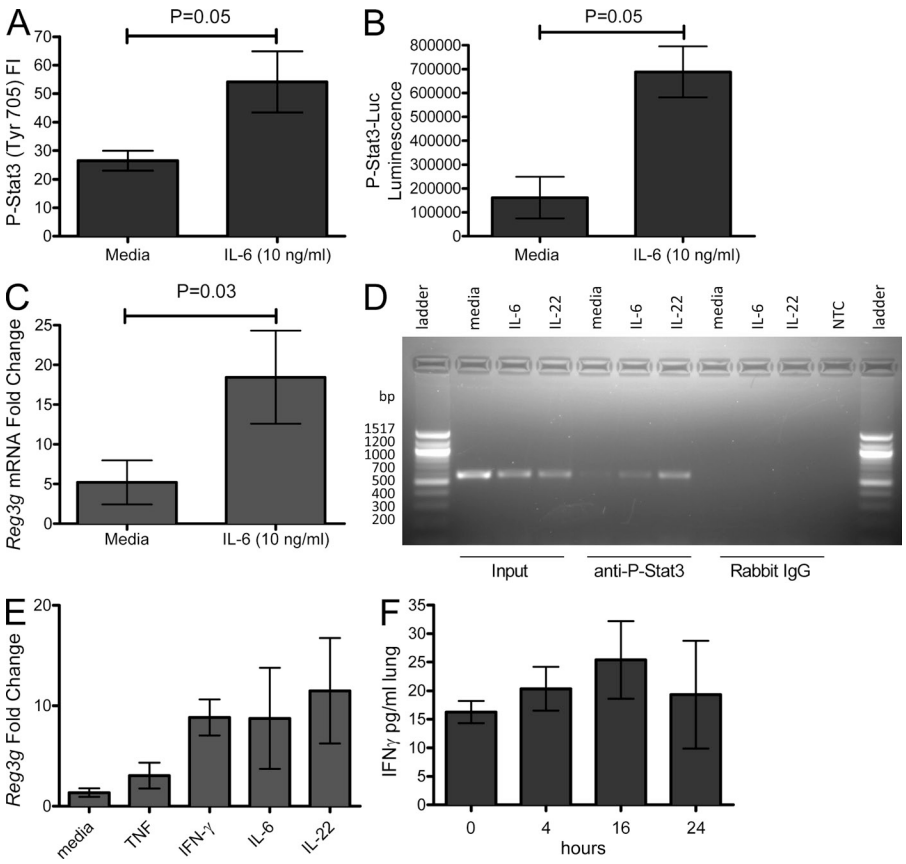

Figure 8. IL-6 stimulation induces P-Stat3 activation and direct transcriptional activation of *Reg3g* expression in MLE12 cells. (A) MLE12 cells respond to IL-6 stimulation and activate Stat3 as determined by increase in fluorescence intensity (FI) in Luminex specific to P-Stat3. (B) IL-6 stimulation of Stat3 signaling is verified by luminescence increase in Stat3-luciferase construct–transduced MLE12 cells 24 h after stimulation. $n = 3$ for each group, independently performed three times. (C) MLE12 cell induction of *Reg3g* in response to IL-6 stimulation is seen by real-time PCR normalized to *Hprt*. $n = 6$ for each group, independently performed twice. (D) Increased P-Stat3 binding to upstream regions of *Reg3g* chromatin of MLE12 cells after 1-h stimulation of 10 ng/ml IL-6 or 50 ng/ml IL-22 is detected by PCR. The second through fourth lanes are PCR of input DNA from nonstimulated or IL-6– or IL-22–stimulated cells, and the fifth through seventh lanes are PCR of DNA after chromatin precipitation with P-Stat3 antibody. (E) MLE12 cells ($n = 3$) were incubated with TNF, IFN-γ, IL-6, or IL-22 for 2 h followed by RNA extraction and assessment of *Reg3g* expression by real-time PCR normalized to *Hprt*. (F) IFN-γ was measured during the time occurs of US300 in lung homogenate of mice ($n = 4$–5 per time point). All levels were <50 pg/mg during this course of infection. P-values by Mann-Whitney test are as indicted. Error bars represent the SE.

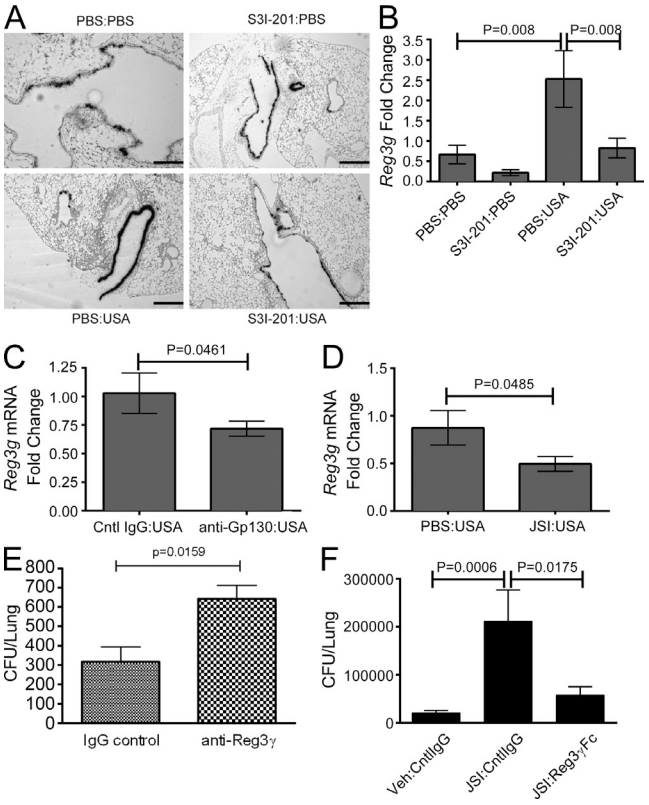

Figure 9. *Reg3g* is induced in the lung epithelium in response to USA300, and Reg3γ rescues Stat3 inhibition of MRSA clearance in vivo. (A) *Reg3g* mRNA production by airway epithelial cells visualized by in situ hybridization of lungs perfused with 10% formalin 24 h after USA300 infection. Bars, 500 µm. (B–D) Stat3-dependent induction of *Reg3g* 16 h after USA300 infection was seen by real-time PCR of *Reg3g* normalized to *Hprt*. $n = 5–10$ for each group, independently performed twice. (E) Intratracheal anti-Reg3γ antibody decreases clearance of USA300 in the lung. (F) Recombinant Reg3γ-Fc (60 µg/mouse) OA administered 4 h after infection rescues increased lung burden of USA300 seen with i.p. JSI-124 Stat3 inhibition at 16 h after infection. $n = 7$ for each group, independently performed twice. P-values by unpaired Student's *t* or Mann-Whitney test are as indicted. Error bars represent the SE.

and specifically binds to the *Reg3g* promoter, IL-22 was dispensable for the in vivo induction of Reg3γ in the lung during USA300 clearance. Moreover, IFN-γ can also induce *Reg3g* in MLE12 cells, but this cytokine was only modestly induced during MRSA pneumonia compared with the Gp130 ligands (Fig. 8, E and F). Gp130 played a significantly greater role in regulating the induction of *Reg3g* in vivo. The pulmonary epithelium employs multiple immune defense strategies and has been under-studied in response to MRSA pneumonia. In addition to providing a physical barrier and using mucociliary clearance to eliminate microbes from the respiratory tract, pulmonary epithelium produces antimicrobial peptides, reactive oxygen species, inflammatory cytokines, and chemokines for neutrophil recruitment (Bals and Hiemstra, 2004). During live pathogen challenge, MyD88 expression by nonhematopoietic cells was required to control early bacteria replication and neutrophil recruitment in response to *Pseudomonas aeruginosa*, whereas hematopoietic MyD88 expression was required at later time points (Skerrett et al., 2004). Our findings suggest that the pulmonary epithelium plays an underappreciated role in early stages of inflammation by expressing the antimicrobial protein Reg3γ.

The role of myeloid versus nonmyeloid cell Stat3 in HIES remains controversial. One study of bone marrow transplantation in a 7-yr-old girl failed to improve the disease despite achieving chimerism in peripheral blood (Gennery et al., 2000). However, successful use of bone marrow transplantation in HIES has been recently reported in two patients, suggesting that some patients with HIES may benefit from bone marrow transplantation (Goussetis et al., 2010). It is important to note that in the MRSA model reported in this paper, the lack of requirement of T, B, or NK cells may be specific to this primary infection model as opposed to secondary lung infections that can occur after colonization of the skin or nasopharynx with SA. However, it is important to understand the contributions of intrinsic Stat3 versus myeloid Stat3 as some HIES patients develop severe enough lung disease to be listed for lung transplantation. Thus, it is critical to determine whether reconstituting intrinsic Stat3 in lung parenchymal cells with a lung transplant is sufficient to correct the pulmonary phenotype. Moreover, most patients with HIES develop infection with methicillin-sensitive SA (MSSA); however, we found that the USA300 strain caused similar induction of IL-6 as MSSA strains. Both MSSA and MRSA are well-known complications of influenza infection (Randolph et al., 2011; Parker and Prince, 2012), and in this setting, Th17 cytokines IL-17 and IL-22 are necessary for host defense against MSSA pneumonia during coinfection with influenza A (Kudva et al., 2011). We hypothesize that the requirement of IL-17 and IL-22 in this model may be caused by compromised epithelial host defenses, and thus epithelial antimicrobial factors may not be available to contain SA.

It is interesting to note that we detected both full-length and cleaved Reg3γ in this model (Fig. 6 C). Full-length Reg3γ protein had bacteriostatic activity, whereas the cleaved protein was bactericidal as has been reported for *L. monocytogenes* (Mukherjee et al., 2009). For these assays, we replicated similar assays as reported for *Listeria* at pH 5.5 (Mukherjee et al., 2009). The airway surface liquid does not become this acidic, and thus future work will be needed to determine how Reg3γ is cleaved in the lung and whether the full-length protein can opsonize USA300 and could possibly be activated in an acidic compartment such as the phagolysosome. In addition to Stat3, we observed induction of Reg3γ by IFN-γ in MLE12 cells, and it has been reported that Stat6 can also regulate Reg3γ expression in the lung (Kuperman et al., 2005). Thus, it appears that other signaling pathways can clearly regulate Reg3γ in vivo, and these alternative signaling pathways could be induced by other components of the lung microbiota. Thus, in HIES patients that may have coinfection, these alternative signaling pathways could potentially compensate for *Reg3g* expression. Future studies will need to determine the regulation of Reg3γ

in more complex coinfection models and determine the contribution of Stat3 in regulating Reg3γ expression under these types of conditions.

Deregulated Stat3 activation is linked to various cancers and poor prognosis, and many Stat3 inhibitors (i.e., JAK2 tyrosine kinase inhibitors and Sunitinib tyrosine kinase inhibitor) are in clinical trials (Yu et al., 2009). Although the use of these therapies for cancer is necessary if proven beneficial, the potential for decreased host immune defense to microbes in these patients has not been determined. In conclusion, Stat3-dependent epithelial production of antimicrobial protein Reg3γ is an essential host defense mechanism against MRSA pneumonia. Furthermore, Reg3γ could be developed to complement antibiotics against multi-drug–resistant SA.

MATERIALS AND METHODS

Mice. Male C57BL/6 (WTB6) 6–8-wk-old mice were obtained from Charles River. *Rag2*$^{-/-}$*/Il2rγ*$^{-/-}$, *Il17ra*$^{-/-}$, and *Il22*$^{-/-}$ mice from Taconic and *Stat3*$^{flx/flx}$ mice from M.H. Kaplan all on C57BL/6 background were bred in specific pathogen–free rooms within animal facilities at the Louisiana State University (LSU) Health Sciences Center. Controls for each experiment were sex and age matched from the same vendor, WTB6 from Charles River and various KOs from Taconic or littermate controls. WTB6 mice were depleted of macrophages or neutrophils by OA 75 µl clodronate (Encapsula) administration 48 h before infection or i.p. 500 µg 1A8 antibody (Bio-XCell) administration 24 h before infection, respectively. Lung burden by CFU counts was determined at 24 h after infection. Gp130 receptor was inhibited by OA 50 µg anti-mGp130 antibody (R&D Systems) immediately before USA300 infection. Stat3 signaling was inhibited by i.p. 1.5 mg/kg JSI-124 (Sigma-Aldrich) or i.p. or OA 5 mg/kg S3I-201 (EMD Millipore) 1 h before USA300 infection. All protocols were approved by the Institutional Animal Care and Use Committee at the LSU Health Sciences Center.

OA of MRSA in mice. A single colony of MRSA USA300 strain (from F. DeLeo, Rocky Mountain Laboratories, National Institute of Allergy and Infectious Diseases, Hamilton, MT) was grown for 18 h at 37°C in 5 ml BBL Trypticase Soy Broth (BD). After this period, fresh TSB media was inoculated with the bacteria at 1:100 dilution and incubated at 37°C for 2 h with shaking to obtain bacteria during log phase of growth. These bacteria were washed with PBS, resuspended in 1 ml PBS, and diluted 5× to obtain ∼4 × 10^8 CFU/ml of working stock. 50 µl of this working stock was administered with tongue pull method at a dose of ∼2 × 10^7 CFU of USA300 in the lung. Working stock was serially diluted and plated on Luria broth plates to determine the exact concentration. For Reg3γ rescue of Stat3 inhibition, recombinant Reg3γ-Fc at a dose of 60 µg was given OA to USA300-administered mice 4 h after infection. For Reg3γ neutralization in vivo, mice received 50 µg of rabbit IgG or Reg3γ antibody OA immediately before USA300.

Lung bacterial burden, mRNA, and protein analysis. Lungs were harvested in PBS, homogenized with a glass homogenizer, and plated on Luria broth in three serial dilutions. Colonies were counted after overnight incubation at 37°C. Gene expression was determined by mRNA extraction with TRIzol (Invitrogen), reverse transcription by iScript (Bio-Rad Laboratories), and qPCR with TaqMan probes (Applied Biosystems) on an iCycler thermal cycler (Bio-Rad Laboratories). All CT values were normalized to *Hprt*. Lung homogenates were analyzed using bead-based Luminex assay (EMD Millipore) for both cytokine and P-Stat3 levels. BALF IL-6 was measured with ELISA (eBioscience). Reg3γ was detected in whole lung homogenate by sandwich ELISA (USCN Life Sciences) in accordance with the protocol provided with the kit.

Immunohistochemistry. The left lung was inflated with 10% neutral buffered formalin for 24 h before paraffin embedding. Slides were stained with P-Stat3 antibodies (Cell Signaling Technology). The number of P-Stat3–positive cells was counted in relation to the total number of epithelial cells in immunohistochemistry lung slides from naive, USA300-infected, and Stat3-inhibited-before-USA300-infection mice.

Reg3γ binding and growth inhibition of MRSA. For binding, overnight cultures of SA USA300 were resuspended in PBS containing recombinant mouse Reg3γ-Fc (provided by W. Ouyang, Genentech, South San Francisco, CA; Zheng et al., 2008) or IgG2a isotype control (BD) for 1 h, followed by goat anti–mouse IgG2a–Alexa Fluor 488 (Invitrogen) for 30 min. Bacteria were fixed with 2% formaldehyde, and flow cytometry was conducted on a FACSCalibur (BD). To assess growth kinetics, overnight cultures were diluted 1:500 in TSB containing isotype control, Reg3γ-Fc, or Reg3γ-Fc with Reg3γ antibody (Abgent), and OD600 readings were measured at hourly intervals.

Reg3γ in BAL. 10 ml BALF was obtained at 20 h after OA administration of USA300 (2 × 10^7 CFU). BALF was concentrated (centrifugal filter; EMD Millipore), and Reg3γ was detected by Reg3γ antisera (Cash et al., 2006) on an SDS-PAGE Western blot (4–12%). Recombinant Reg3γ-Fc protein was used as positive control.

MLE12 cell culture and IL-6 stimulation. MLE12 (CRL-2110; American Type Culture Collection) was regularly passed in DMEM/F12 medium supplemented with 1.94 mM L-glutamine, 10 mM Hepes, 5 µg/ml insulin, 10 µg/ml transferring, 10 nM hydrocortisone, 10 mM β-estradiol, penicillin, streptomycin, and 2% fetal bovine serum. Cells were seeded at 2 × 10^6 cells/ml in 24-well plates 1 d before stimulation. Cells were stimulated with 10 ng/ml IL-6 (R&D Systems) for 15 min for P-Stat3 Luminex (EMD Millipore) and 2 h for *Reg3g* mRNA (TRIzol; Applied Biosystems). MLE12 cells were stably transduced with P-Stat3–Luciferase by lentiviral construct (SA-Biosciences). Luminescence reading (Promega) was taken at 24 h after stimulation with 10 ng/ml IL-6.

ChIP. MLE12 cells were stimulated with 10 ng/ml IL-6 for 1 h before cross-linking with 37% formaldehyde. ChIP assay was performed with P-Stat3 antibody (Cell Signaling Technology) at 1:50 dilution along the EZ-ChIP kit (EMD Millipore) protocol. Normal rabbit IgG antibody (Cell Signaling Technology) was used as negative control for polyclonal rabbit P-Stat3 antibody. 50-cycle standard PCR was performed with 5′-ATGCTCATGCAAGTCAGGGAGGTA-3′ and 5′-GCAGCAGGAAAGCAAGTCCATTCT-3′ primers (IDT), flanking the 577-bp area −650 to −80 bp upstream of the *Reg3g* start site.

In situ hybridization. The mouse *Reg3g* cDNA was amplified by PCR using gene-specific primers designed based on mouse sequences available in GenBank (accession no. NM_011260). The primer sequences were SQ_mReg3g_F1, 5′-GATGCTTCCCCGTATAACCATCACCA-3′; and SQ_mReg3g_R1, 5′-CTAGGCCTTGAATTTGCAGACATAGGGT-3′. The template used for amplification was a plasmid containing a Reg3γ-Fc construct. The amplified products were ligated into pGEMT vector (Promega) and DNA sequenced. The Vector NTI Advance software package (Invitrogen) was used for analysis of the resulting DNA sequences. We performed stringent in situ hybridization (21-d exposures) as described previously (Reinhart et al., 2002).

Reg3γ ELISA. Lung homogenates from naive WTB6 and *Rag2/Il2rg*$^{-/-}$ mice were diluted in 0.1 M carbonate coating buffer and plated in 96-well Nunc MaxiSorp plates (Thermo Fisher Scientific) overnight at 4°C. The next day, plates were washed with PBS containing 0.05% Tween, blocked with PBS containing 5% milk, and incubated with rabbit anti-Reg3γ serum for 2 h (provided by L. Hooper, University of Texas Southwestern Medical Center, Dallas, TX; Cash et al., 2006) Plates were then washed, incubated with anti–rabbit IgG-HRP (Cell Signaling Technology) for 1 h, washed, and developed using 1× TMB substrate (eBioscience). Recombinant mouse

Reg3γ-Fc was used as a standard. Reg3γ expression was also confirmed and quantified using a commercial sandwich ELISA (USCN Life Sciences)

Bactericidal assays. Bactericidal assays were performed as previously described (Cash et al., 2006). In brief, SA was grown for 8 h in brain heart infusion broth (Sigma-Aldrich) and diluted 1:100 into buffer containing recombinant mouse Reg3γ-Fc or Reg3γ-cleaved (10 mM MES and 25 mM NaCl, pH 5.5). Bacteria were incubated with shaking at 37°C for 2 h, and then serial dilutions were plated on brain heart infusion agar for CFU analysis.

We would like to thank Dr. Lora Hooper for the Reg3γ antisera and cleaved Reg3γ, Dr. Frank DeLeo for the MRSA USA300 strain, and Dr. Wenjun Ouyang for the Reg3γ-Fc construct and protein.

This work was supported by the Public Health Service grant R37-HL079142.

The authors have no competing financial interests.

Submitted: 4 June 2012
Accepted: 14 January 2013

REFERENCES

Bals, R., and P.S. Hiemstra. 2004. Innate immunity in the lung: how epithelial cells fight against respiratory pathogens. *Eur. Respir. J.* 23:327–333. http://dx.doi.org/10.1183/09031936.03.00098803

Cash, H.L., C.V. Whitham, and L.V. Hooper. 2006. Refolding, purification, and characterization of human and murine RegIII proteins expressed in *Escherichia coli*. *Protein Expr. Purif.* 48:151–159. http://dx.doi.org/10.1016/j.pep.2006.01.014

Cho, J.S., E.M. Pietras, N.C. Garcia, R.I. Ramos, D.M. Farzam, H.R. Monroe, J.E. Magorien, A. Blauvelt, J.K. Kolls, A.L. Cheung, et al. 2010. IL-17 is essential for host defense against cutaneous *Staphylococcus aureus* infection in mice. *J. Clin. Invest.* 120:1762–1773. http://dx.doi.org/10.1172/JCI40891

David, M.Z., and R.S. Daum. 2010. Community-associated methicillin-resistant *Staphylococcus aureus*: epidemiology and clinical consequences of an emerging epidemic. *Clin. Microbiol. Rev.* 23:616–687. http://dx.doi.org/10.1128/CMR.00081-09

Defres, S., C. Marwick, and D. Nathwani. 2009. MRSA as a cause of lung infection including airway infection, community-acquired pneumonia and hospital-acquired pneumonia. *Eur. Respir. J.* 34:1470–1476. http://dx.doi.org/10.1183/09031936.00122309

DeLeo, F.R., M. Otto, B.N. Kreiswirth, and H.F. Chambers. 2010. Community-associated meticillin-resistant *Staphylococcus aureus*. *Lancet*. 375:1557–1568. http://dx.doi.org/10.1016/S0140-6736(09)61999-1

Gennery, A.R., T.J. Flood, M. Abinun, and A.J. Cant. 2000. Bone marrow transplantation does not correct the hyper IgE syndrome. *Bone Marrow Transplant.* 25:1303–1305. http://dx.doi.org/10.1038/sj.bmt.1702446

Goussetis, E., I. Peristeri, V. Kitra, J. Traeger-Synodinos, M. Theodosaki, K. Psarra, M. Kanariou, F. Tzortzatou-Stathopoulou, E. Petrakou, I. Fylaktou, et al. 2010. Successful long-term immunologic reconstitution by allogeneic hematopoietic stem cell transplantation cures patients with autosomal dominant hyper-IgE syndrome. *J. Allergy Clin. Immunol.* 126:392–394. http://dx.doi.org/10.1016/j.jaci.2010.05.005

Graham, P.L. III, S.X. Lin, and E.L. Larson. 2006. A U.S. population-based survey of *Staphylococcus aureus* colonization. *Ann. Intern. Med.* 144:318–325.

Heimall, J., A. Freeman, and S.M. Holland. 2010. Pathogenesis of hyper IgE syndrome. *Clin. Rev. Allergy Immunol.* 38:32–38. http://dx.doi.org/10.1007/s12016-009-8134-1

Klevens, R.M., M.A. Morrison, J. Nadle, S. Petit, K. Gershman, S. Ray, L.H. Harrison, R. Lynfield, G. Dumyati, J.M. Townes, et al; Active Bacterial Core surveillance (ABCs) MRSA Investigators. 2007. Invasive methicillin-resistant *Staphylococcus aureus* infections in the United States. *JAMA*. 298:1763–1771. http://dx.doi.org/10.1001/jama.298.15.1763

Kudva, A., E.V. Scheller, K.M. Robinson, C.R. Crowe, S.M. Choi, S.R. Slight, S.A. Khader, P.J. Dubin, R.I. Enelow, J.K. Kolls, and J.F. Alcorn. 2011. Influenza A inhibits Th17-mediated host defense against bacterial pneumonia in mice. *J. Immunol.* 186:1666–1674. http://dx.doi.org/10.4049/jimmunol.1002194

Kuehnert, M.J., D. Kruszon-Moran, H.A. Hill, G. McQuillan, S.K. McAllister, G. Fosheim, L.K. McDougal, J. Chaitram, B. Jensen, S.K. Fridkin, et al. 2006. Prevalence of *Staphylococcus aureus* nasal colonization in the United States, 2001-2002. *J. Infect. Dis.* 193:172–179. http://dx.doi.org/10.1086/499632

Kuperman, D.A., C.C. Lewis, P.G. Woodruff, M.W. Rodriguez, Y.H. Yang, G.M. Dolganov, J.V. Fahy, and D.J. Erle. 2005. Dissecting asthma using focused transgenic modeling and functional genomics. *J. Allergy Clin. Immunol.* 116:305–311. http://dx.doi.org/10.1016/j.jaci.2005.03.024

Matsuzaki, Y., Y. Xu, M. Ikegami, V. Besnard, K.S. Park, W.M. Hull, S.E. Wert, and J.A. Whitsett. 2006. Stat3 is required for cytoprotection of the respiratory epithelium during adenoviral infection. *J. Immunol.* 177:527–537.

Miller, L.S., E.M. Pietras, L.H. Uricchio, K. Hirano, S. Rao, H. Lin, R.M. O'Connell, Y. Iwakura, A.L. Cheung, G. Cheng, and R.L. Modlin. 2007. Inflammasome-mediated production of IL-1beta is required for neutrophil recruitment against *Staphylococcus aureus* in vivo. *J. Immunol.* 179:6933–6942.

Minegishi, Y., M. Saito, M. Nagasawa, H. Takada, T. Hara, S. Tsuchiya, K. Agematsu, M. Yamada, N. Kawamura, T. Ariga, et al. 2009. Molecular explanation for the contradiction between systemic Th17 defect and localized bacterial infection in hyper-IgE syndrome. *J. Exp. Med.* 206:1291–1301. http://dx.doi.org/10.1084/jem.20082767

Mukherjee, S., C.L. Partch, R.E. Lehotzky, C.V. Whitham, H. Chu, C.L. Bevins, K.H. Gardner, and L.V. Hooper. 2009. Regulation of C-type lectin antimicrobial activity by a flexible N-terminal prosegment. *J. Biol. Chem.* 284:4881–4888. http://dx.doi.org/10.1074/jbc.M808077200

Napolitano, L.M., M.E. Brunsvold, R.C. Reddy, and R.C. Hyzy. 2009. Community-acquired methicillin-resistant *Staphylococcus aureus* pneumonia and ARDS: 1-year follow-up. *Chest.* 136:1407–1412. http://dx.doi.org/10.1378/chest.07-1511

Parker, D., and A. Prince. 2012. Immunopathogenesis of *Staphylococcus aureus* pulmonary infection. *Semin. Immunopathol.* 34:281–297. http://dx.doi.org/10.1007/s00281-011-0291-7

Pickert, G., C. Neufert, M. Leppkes, Y. Zheng, N. Wittkopf, M. Warntjen, H.A. Lehr, S. Hirth, B. Weigmann, S. Wirtz, et al. 2009. STAT3 links IL-22 signaling in intestinal epithelial cells to mucosal wound healing. *J. Exp. Med.* 206:1465–1472. http://dx.doi.org/10.1084/jem.20082683

Quinton, L.J., M.R. Jones, B.E. Robson, B.T. Simms, J.A. Whitsett, and J.P. Mizgerd. 2008. Alveolar epithelial STAT3, IL-6 family cytokines, and host defense during *Escherichia coli* pneumonia. *Am. J. Respir. Cell Mol. Biol.* 38:699–706. http://dx.doi.org/10.1165/rcmb.2007-0365OC

Randolph, A.G., F. Vaughn, R. Sullivan, L. Rubinson, B.T. Thompson, G. Yoon, E. Smoot, T.W. Rice, L.L. Loftis, M. Helfaer, et al; Pediatric Acute Lung Injury and Sepsis Investigator's Network and the National Heart, Lung, and Blood Institute ARDS Clinical Trials Network. 2011. Critically ill children during the 2009-2010 influenza pandemic in the United States. *Pediatrics.* 128:e1450–e1458. http://dx.doi.org/10.1542/peds.2011-0774

Reinhart, T.A., B.A. Fallert, M.E. Pfeifer, S. Sanghavi, S. Capuano III, P. Rajakumar, M. Murphey-Corb, R. Day, C.L. Fuller, and T.M. Schaefer. 2002. Increased expression of the inflammatory chemokine CXC chemokine ligand 9/monokine induced by interferon-gamma in lymphoid tissues of rhesus macaques during simian immunodeficiency virus infection and acquired immunodeficiency syndrome. *Blood.* 99:3119–3128. http://dx.doi.org/10.1182/blood.V99.9.3119

Skerrett, S.J., H.D. Liggitt, A.M. Hajjar, and C.B. Wilson. 2004. Cutting edge: myeloid differentiation factor 88 is essential for pulmonary host defense against *Pseudomonas aeruginosa* but not *Staphylococcus aureus*. *J. Immunol.* 172:3377–3381.

Small, C.L., S. McCormick, N. Gill, K. Kugathasan, M. Santosuosso, N. Donaldson, D.E. Heinrichs, A. Ashkar, and Z. Xing. 2008. NK cells play a critical

protective role in host defense against acute extracellular *Staphylococcus aureus* bacterial infection in the lung. *J. Immunol.* 180:5558–5568.

Vaishnava, S., M. Yamamoto, K.M. Severson, K.A. Ruhn, X. Yu, O. Koren, R. Ley, E.K. Wakeland, and L.V. Hooper. 2011. The antibacterial lectin RegIIIgamma promotes the spatial segregation of microbiota and host in the intestine. *Science*. 334:255–258. http://dx.doi.org/10.1126/science.1209791

von Köckritz-Blickwede, M., M. Rohde, S. Oehmcke, L.S. Miller, A.L. Cheung, H. Herwald, S. Foster, and E. Medina. 2008. Immunological mechanisms underlying the genetic predisposition to severe *Staphylococcus aureus* infection in the mouse model. *Am. J. Pathol.* 173:1657–1668. http://dx.doi.org/10.2353/ajpath.2008.080337

Xu, Y., M. Ikegami, Y. Wang, Y. Matsuzaki, and J.A. Whitsett. 2007. Gene expression and biological processes influenced by deletion of Stat3 in pulmonary type II epithelial cells. *BMC Genomics*. 8:455. http://dx.doi.org/10.1186/1471-2164-8-455

Yu, H., D. Pardoll, and R. Jove. 2009. STATs in cancer inflammation and immunity: a leading role for STAT3. *Nat. Rev. Cancer*. 9:798–809. http://dx.doi.org/10.1038/nrc2734

Zheng, Y., P.A. Valdez, D.M. Danilenko, Y. Hu, S.M. Sa, Q. Gong, A.R. Abbas, Z. Modrusan, N. Ghilardi, F.J. de Sauvage, and W. Ouyang. 2008. Interleukin-22 mediates early host defense against attaching and effacing bacterial pathogens. *Nat. Med.* 14:282–289. http://dx.doi.org/10.1038/nm1720